Article

Effect of Mg and Nano-TiO_2 on the Marine Protective Properties of Zn-Al Coatings

Kunkun Wang[1], Shouren Wang[1,*], Tianying Xiong[2], Daosheng Wen[1], Gaoqi Wang[1] , Wentao Liu[1] and Hao Du [2]

[1] School of Mechanical Engineering, University of Jinan, Jinan, 250022, China;

495286093@qq.com (K.W.); me_wends@ujn.edu.cn (D.W.); me_wanggq@ujn.edu.cn (G.W.); me_liuwt@ujn.edu.cn(W.L.)

[2] Institute of Metal Research, Chinese Academy of Sciences, Shenyang, 110016, China;

tyxiong@imr.ac.cn (T.X.); hdu @ imr.ac.cn (H.D.)

* Correspondence: me_wangsr@ujn.edu.cn (S.W.)

Abstract: According to research, we have learned that Mg and TiO_2 are new types material of marine protective coatings. We found that the addition of Mg can improve the performance of Zn-Al coating passivation film, and TiO_2 has excellent photocatalytic self-cleaning performance. In this paper Zn-Al pseudo alloy coating was prepared by cold spray technique, and Zn-Al-Mg-TiO_2 pseudo alloy composite coating was prepared by adding Mg and nano-TiO_2. The effects of Mg and TiO_2 to the marine protective properties of Zn-Al coatings were studied by friction and wear test, dynamic salt water corrosion test, electrochemical test, scanning electron microscope(SEM), energy dispersive spectrometer(EDS) and super deep scene 3D microscope. The results show that the addition of Mg and nano-TiO_2 not only fills the gap of the coating and improves the density of the coating, but also generates grid-like flocculent corrosion products on the surface of the coating which can gather other corrosion products to improve the density of corrosion products, reduce the friction coefficient and corrosion rate of the coating surface, effectively prevent the invasion of Cl^- in solution, and improve the wear and corrosion resistance of the coating.

Keywords: Zn-Al-Mg-TiO_2 coating; Zn-Al coating; Marine anticorrosion; corrosion; Friction and wear

1. Introduction

In the field of anticorrosive coatings for marine equipment, Zn-Al series coatings are the focuses of current research[1]. As early as the 1920s, research on Zn-Al protective coatings has been carried out abroad and applied in practice[2]. It was found that the Zn-Al alloy coating combines the advantages of Zn coating and Al coating. Zn-Al coating not only has excellent electrochemical cathodic protection performance of pure Zn coating, but also forms corrosion passivation film on the surface of the coating when addition of Al element which can effectively slows down the corrosion rate[3-5].

In recent years, people have tried to add Mg element to Zn-Al coatings for research which can significantly improve the corrosion resistance of the coatings[6-8]. Yao et al through the study of Zn-Al-Mg coating prepared by hot dipping, It was found that the addition of magnesium can not only improve the microhardness of the coating, but also form special corrosion products, block the passage of oxygen and water, and reduce the corrosion rate[9]. Joung et al, study Zn-Mg coatings and found addition of magnesium resulted in the change of coating structure and corrosion product film which had better corrosion resistance than pure zinc coatings[10].

TiO_2 is a newly marine antifouling and self-cleaning material with excellent chemical stability[11-13]. TiO_2 has excellent self-cleaning effect because it can react to produce hydroxyl groups under light which can form a physical adsorption layer on the surface. In addition, its own nanostructure has a certain shielding effect. Therefore, it has a good application prospect in the field of marine equipment anti-fouling[14-17]. Nano-TiO_2 was successfully added to varnish in Ford Central Laboratory, USA, to obtain coatings with good weatherability and scratch resistance [16].

Therefore, this paper intends to prepare Zn-Al-Mg-TiO_2 coating by cold spraying. Then study the effect of Mg and TiO_2 addition to the corrosion resistance of Zn-Al coating with experiments, and discuss the anti-corrosion mechanism of Zn-Al-Mg-TiO_2 coating, so as to provide some reference for further research of marine metal anti-corrosion coating.

2. Experimental processes

2.1. Preparation of coatings

100μm Zn-Al and Zn-Al-Mg-TiO_2 coatings were prepared on a 200x30x3mm Q235 substrate by cold spraying equipment. The working parameters of cold spraying are as follows: (1) The working gas is ordinary compressed air with pressure 2MPa and temperature 300 ℃; (2) The distance between the spray nozzle and the base is 20 mm. (3) The moving speed of the spray nozzle is 2 mm/s.

The sample is cut into 10 x 10 x 3 mm pieces by wire electrical discharge machining(WEDM) and ground with 800, 1000, 1500, 2000 and 2500 meshes of sandpaper, then the specimens were decontaminated and degreased by ultrasonic in alcohol.

2.2. Testing and Analysis of Coatings

In order to compare the effect of Mg and nano-TiO_2 to the corrosion resistance of Zn-Al coating and study its advantages, we through the immersion test in dynamic salt water, friction and wear test and electrochemical test to test and prove.

In order to simulate the marine environment, the CJJ79-1 magnetic stirrer was used to stir the corrosive medium for the dynamic salt water corrosion test. Other uncoated surfaces of the sample are covered by silicone rubber resin and the corrosive medium is 3.5% NaCl solution, The samples were corroded in solution for 144h, 240h, 480h and 720h.

Reciprocate friction wear test of two coatings used RTEC friction and wear tester, and the working parameters were as follows: Loading force was 20N, reciprocating frequency was 4HZ and friction pair was Q235 with 20 minutes. After the test, measured the wear extent of the sample by electronicbalance.

The electrochemical test was carried out using CHI604E electrochemical workstation. Before the test, other uncoated surfaces of the sample are covered by silicone rubber resin. Then the open circuit potential and tafel polarisation curves plot of samples was tested who immersed in 3.5% NaCl solution for different time periods. In addition the initial potential, the final potential, and the scan rate of the tafel polarisation curves plot were -1.8 V, -0.8 V, and 10 mv / s, respectively.

Using super deep scene 3D microscope, electrochemical test, scanning electron microscope(SEM) and energy dispersive spectrometer(EDS) to characterize the composition and surface micro-morphology of sample when the test resule was analysised.

3. Results

3.1. Surface appearance and characterization

The surface micro-morphology and EDS analysis of Zn-Al coating and Zn-Al-Mg-TiO_2 composite coating are shown in Fig.1. We can see that the coating materials are distributed in groups.

The brighter colour is the zinc-rich group and the darker colour is the aluminium-rich group. As shown in fig.1 (a), there are many holes and pits on the surface of Zn-Al coating, and the distribution of material groups is concentrated and not uniform enough. As depicted by Fig.1(b) the interlaced distribution of material groups in Zn-Al-Mg-TiO_2 coating is more uniform, and the content of Mg is less so distributed more dispersed. TiO_2 particles are widely distributed among the groups because of its small size, it fills in the pore and crack of the coating, so the surface is smooth. Compared with the Zn-Al coating, the structure of the Zn-Al-Mg-TiO_2 composite coating is more uniform and compact, with fewer pits and voids and more compact.

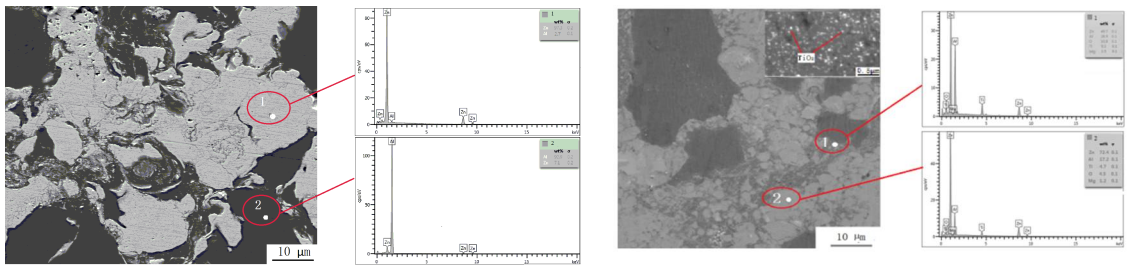

(**a**) (**b**)

Figure 1. The micro-morphology and EDS energy spectrum of coating: (a)Zn-Al coating; (b) Zn-Al-Mg-TiO_2 coating

3.2 *Analysis the wear resistance of coating*

There are two main forms of damage to the rapid consumption of protective coatings on the surface of marine steel substrates. The first is high-salinity marine environmental electrochemical corrosion, the other is the wear that was caused by marine foreign matter and other equipment directly contact with coating[17-18]. No matter which form of damage, it will speed up the consumption of coating and shorten the protection period. Therefore we verified the wear resistance of the coating through the friction and wear test. Fig. 2 shows the friction coefficient curve of reciprocating friction 20 min between the two coatings and Q235 steel ball at 20N and 4HZ frequency. Fig. 3 is a 3D micrograph of the two types coating wear marks. From Fig. 2 we can get the friction coefficient of Zn-Al coating is 0.3750, while the Zn-Al-Mg-TiO_2 coating has a lower friction coefficient than Zn-Al coating which is 0.3601. Besides, the wear extent difference of them is 0.4 mg.

From Fig. 3.3, we can see that the wear scar of Zn-Al-Mg-TiO_2 coating is denser and uniform, and the bottom of the wear marks were relatively flat with a depth of 69.89μm, while the wear marks of The Zn-Al coating are rough and uneven, the fluctuation is large and the deepest place reaches 87.38μm. Therefore, the addition of magnesium and titanium dioxide enables the coating to be uniformly wear under the external force friction and the wear resistance is more excellent.

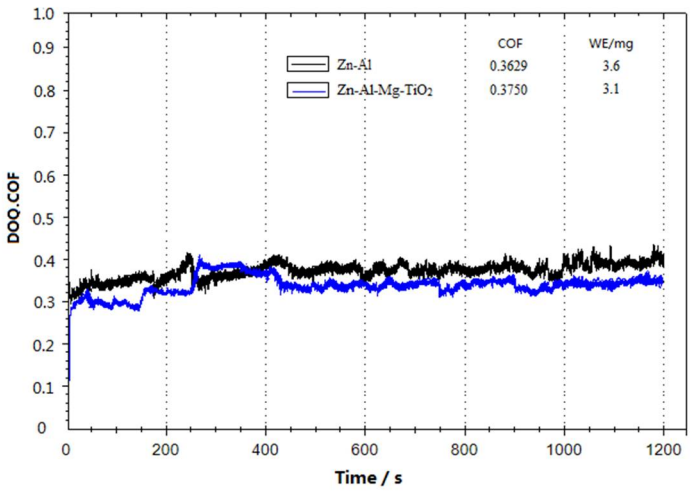

Figure 2. The friction coefficient curve of two coatings

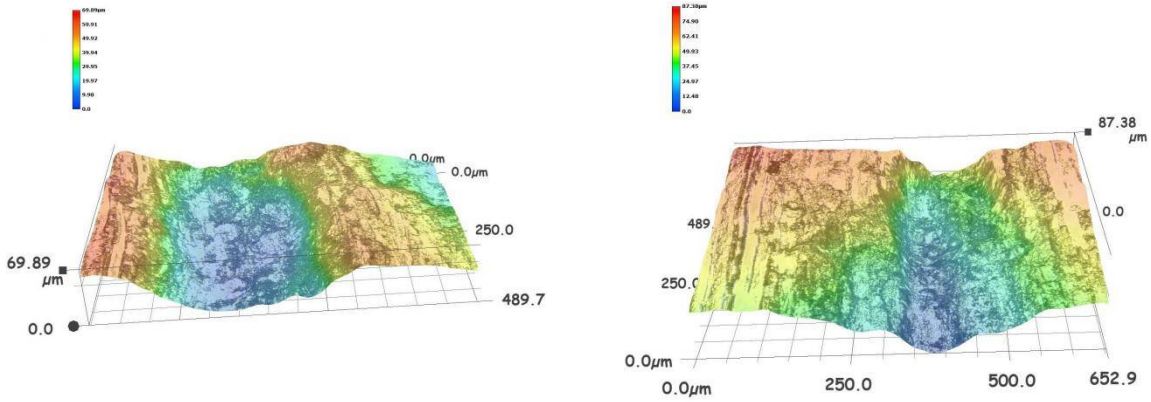

(**a**) (**b**)

Figure 3. Three-dimensional micrograph of two coating wear marks: (a)Zn-Al-Mg-TiO_2 coating; (b)Zn-Al coating

3.3 Analysis of results of the dynamic salt water corrosion test.

Compared with friction and wear, the biggest damage of steel components in the marine environment is the electrochemical erosion of the matrix by halogen ions in sea water[18-19]. In order to understand the corrosion mechanism of the coating in seawater more intuitively, we observe and analyze the sample immersed different stages in the continuously fluctuating 3.5% NaCl solution. Fig. 4 shows the surface macro-morphology of Zn-Al coating and Zn-Al-Mg-TiO_2 composite coating immersed in dynamic salt water for 144 h, 240 h, 480 h and 720 h respectively. As shown in Fig. 4a, the coating of Zn-Al is covered with white corrosive product after immersing 144h. As the immersion time increases, the area of white corrosive material covers gradually increase and thick, and the phenomenon of material falling off occurs. When the white corrosive material falls off, the coating peels off and pits are generated.

As shown in Fig.4(b). The corrosion resistance of Zn-Al-Mg-TiO_2 composite coating is obviously better than Zn-Al coating. At the initial stage of the immersion, there is no adhesion of white corrosion products and a dense corrosion product is formed on the surface, the surface of the coating is smooth. The surface of the composite coating is covered with a thinner layer of white corrosive

product after immersing for 480 hours. At this time, the surface of the coating is still smooth, and there are no large pits. After immersing for 720 hours, the white corrosion fall off from the composite coating surface, but the coating itself material peel off less and has not produced large pits.

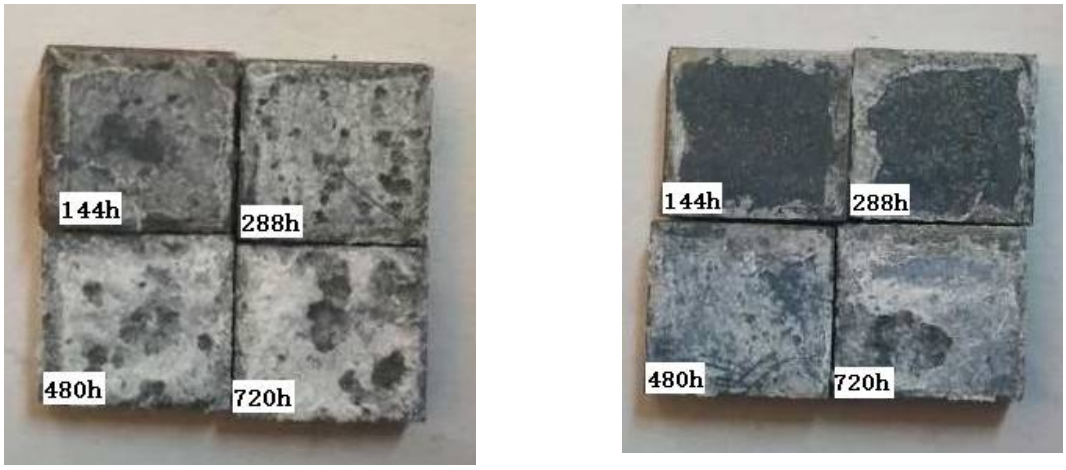

(**a**) (**b**)

Figure 4. The surface macro-morphology of tow types coating immersed in dynamic salt water for 144 h, 240 h, 480 h and 720 h respectively: (a)Zn-Al coating; (b) Zn-Al-Mg-TiO_2 coating

As shown in Fig. 5 and Fig 6, in order to understand the protective mechanism of the coating, the surface topography of the two coatings after different corrosion times was observed by scanning electron microscopy(SEM). By observing fig.5 (a), we can see that the surface of the Zn-Al coating is almost covered by light-colored spherical substances and a dense dark-colored substance is formed between the gap of light-colored spherical substances. Increasing the magnification we can find that the interior of the spherical substances and the gaps of the spherical substances are lamellar substance（fig5（a1）and fig5（a2）. This polygonal layered material with densely structure is a typical corrosion morphology of zinc alloy coating[20]. From the EDS spectrum of the corrosion product of Zn-Al coating in Fig.7, we can find that although the inner and outer parts of the spherical substances are lamellar substance, the Zn, O, Cl and Na elements in the spherical substances are obviously more than the surrounding. However, Al elements in spherical substances are very few. This phenomenon can be explained that the surface of the spherical substances is covered with Zn-rich substance, and the corrosion reaction mainly occurs in this area. During this period, the active metal Zn acts as an anode, providing cathodic protection for other areas by consuming itself. As shown in fig5(b) and (c), with the immersion time prolongs, the spherical substances are gradually decreasing from the surfaces of the Zn-Al coatings. After 720h the surface of the Zn-Al coatings are filled with lamellar corrosion products and generate a large number of cracks(fig5(d)).

However, as shown in fig6 the corrosion resistance of Zn-Al-Mg-TiO2 coating is significantly better than Zn-Al coating. in the first stage of immersion(fig6(a)), the surface of the Zn-Al-Mg-TiO2 composite coating generates little corrosion, and only a part of the position produces lamellar substance. At this time,there is relatively clean and smooth of the coating surface. After 240 hours of immersion, the surface of Zn-Al-Mg-TiO2 composite coating also produces spherical substances, and the gaps between them are filled with lamellar corrosion products(fig6(b)). By comparing Fig. 5(a1) and fig6(a1), we can find that the density of both the spherical substances and lamellar substances of the Zn-Al-Mg-TiO2 is much better than that of the Zn-Al coating. Fig6(c1) is a partial

enlarged view of Fig. 6(c), we can see that there is a grid-like floc morphology under the lamellar substance of Zn-Al-Mg-TiO2. What is more, as shown in fig6(d1) a large number of corrosion products block the surface pores of the grid-like floc morphology, resulting in a dense structure of the corrosion product passivation film formed, which effectively preventing the further invasion of chloride ions. With the immersion time prolongs, the spherical substances are gradually decreasing and a large number of holes appear of the Zn-Al-Mg-TiO2 coating surface, but no obvious crack is generated. After 720h, the main morphology of the surface of Zn-Al-Mg-TiO2 coating is honeycomb-like and the reason for this morphology is that a large amount of Zn had reacted at the beginning of the corrosion and the consumed zinc group generates pores in situ.

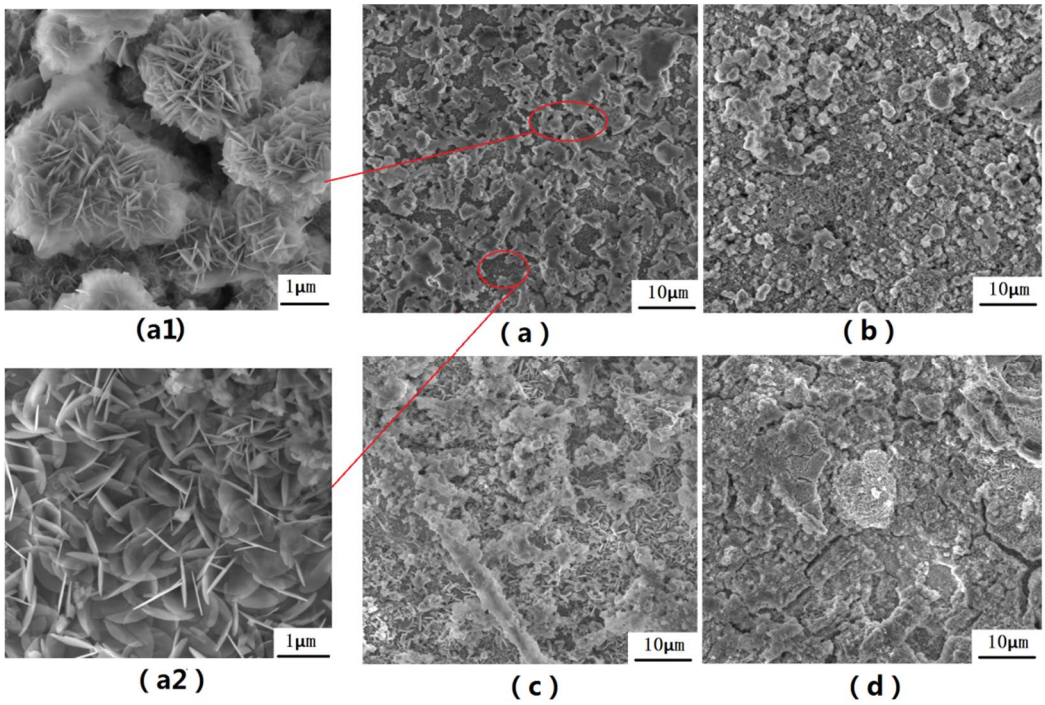

Figure 5. Microscopic topography of the Zn-Al coatings corrosion in the salt water for four periods : (a)Corrosion 144h; (b)Corrosion 240h; (c)Corrosion 480h; (d)Corrosion 720h; (e)Partial enlargement of the spherical substances; (f)Partial enlargement of the lamellar substance

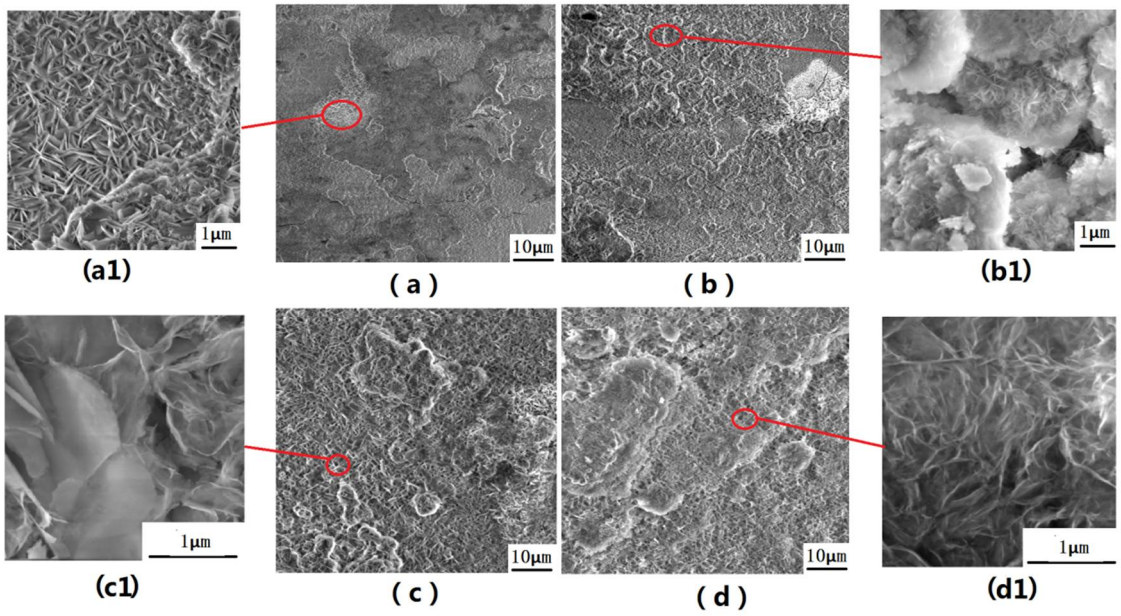

Figure 6. Microscopic topography of the Zn-Al-Mg-TiO_2 coatings corrosion in the salt water for four periods : (a)Corrosion 144h; (b)Corrosion 240h; (c)Corrosion 480h; (d)Corrosion 720h; (e)Partial enlargement of the (a); (f)Partial enlargement of the (c); (g) Partial enlargement of the (b); (h)Partial enlargement of the (d)

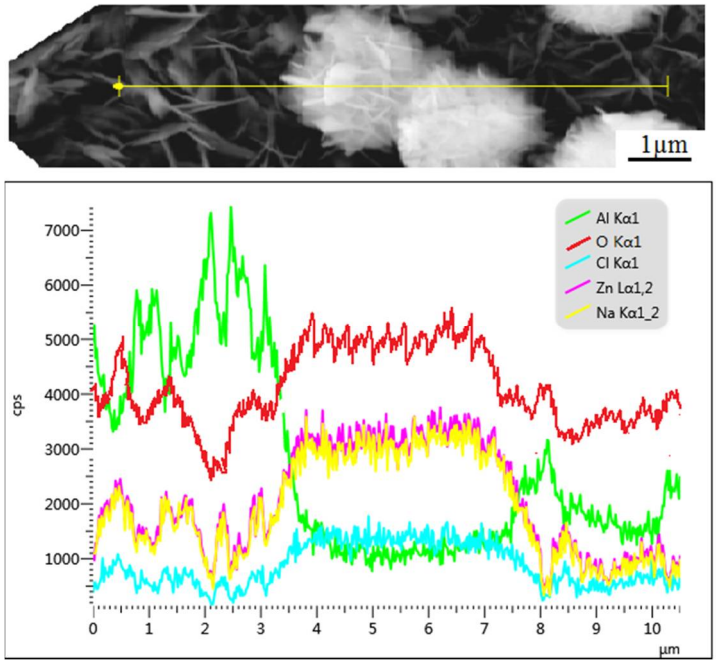

Figure 7. EDS spectrum of corrosion products of Zn-Al coating

3.4 Electrochemical test analysis

191 The zinc and aluminum series coating is a consumable coating that protects the substrate by
192 consuming oneself in the coating reaction with halogen ions.

193 Fig.8 is a graph showing the open circuit potential-time changing trend of Zn-Al coating and
194 Zn-Al-Mg-TiO_2 composite coating in a 3.5% NaCl solution. From the figure, we can see that the open
195 circuit potentials of the two coatings have a same trend with time. In the initial stage of immersion,
196 the open circuit potential of the coating around -1V which is relatively low. The potential changes
197 sharply to -1.35 ~ -1.38V with time, then slowly shifts positively, and finally reaches a dynamic
198 equilibrium. The mainly reason for this phenomenon is the presence of an oxide film on the surface
199 of the initial of corrosion, the electrochemical reaction rate is slow, and the open circuit potential of
200 the coating is relatively low. As the reaction continues, the exposed coating area gradually increases,
201 the mainly reaction at this time is anodic corrosion of zinc, aluminum and magnesium active metals.
202 In this stage the reaction speed of coating is faster and the potential is rapidly move to negative
203 direction. In the later stage of corrosion, dense corrosion products and passivation film on the
204 surface of the coating prevent further immersion of Cl^-, so the open circuit potential moves to the
205 positive direction. Finally, as the corrosion product continues to form, the potentials of the two
206 coatings reach a stable state, but the open circuit potential of Zn- Al-Mg-TiO_2 composite coating has a
207 small fluctuation range and is more stable.

208 Fig.9 is a graph showing the tafel polarisation curves plot of Zn-Al coatings and Zn-
209 Al-Mg-TiO2 composite coatings in 3.5% NaCl solution at different times. Tables 1 and 2 show the
210 corrosion potential and corrosion current density obtained from the polarization curves of the two
211 coatings. We can see that the polarization potentials of both coatings are in the negative direction of
212 the polarization potential of the Q235 substrate, so both of them can provide good electrochemical
213 protection for the substrate. With the change of corrosion time, the corrosion current density of the
214 two coatings increased first and then decreased. It indicates that the corrosion rate of the two
215 coatings are gradually increased at the beginning of corrosion. As the immersion time increases,
216 when the corrosion progresses to a certain extent, the corrosion rate stops increasing and begins to
217 gradually decrease. This phenomenon proves the above judgment. In the initial stage of corrosion, as
218 the oxide film on the surface of the coating decreases, the exposed active metal gradually increases,
219 so the reaction speed increases. As the corrosion progresses, the corrosion products on the surface of
220 the coating gradually increase, and the active metal is covered again, so the corrosion rate is
221 gradually reduced. However, under this trend, the corrosion current density of Zn-Al-Mg-TiO_2
222 coating is always lower than that of Zn-Al coating, indicating the grid-like floc corrosion products
223 formed by adding Mg (Fig 6(d1)) and the TiO_2 nanoparticles filled into the gap can improve the
224 passivation film of the coating which can effectively prevent Cl^- further intrusion and improves the
225 corrosion resistance of the coating.

226

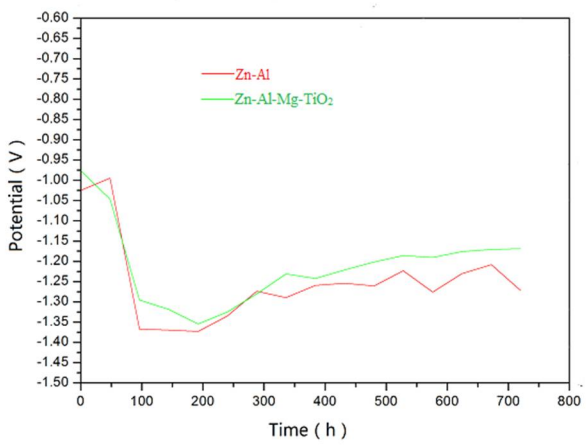

227

Peer-reviewed version available at Coatings 2019, 9, 339; doi:10.3390/coatings9050339

Figure 8. The time-opening potential line chart of Zn-Al coating and Zn-Al-Mg-TiO_2 composite coating in 3.5% NaCl solution

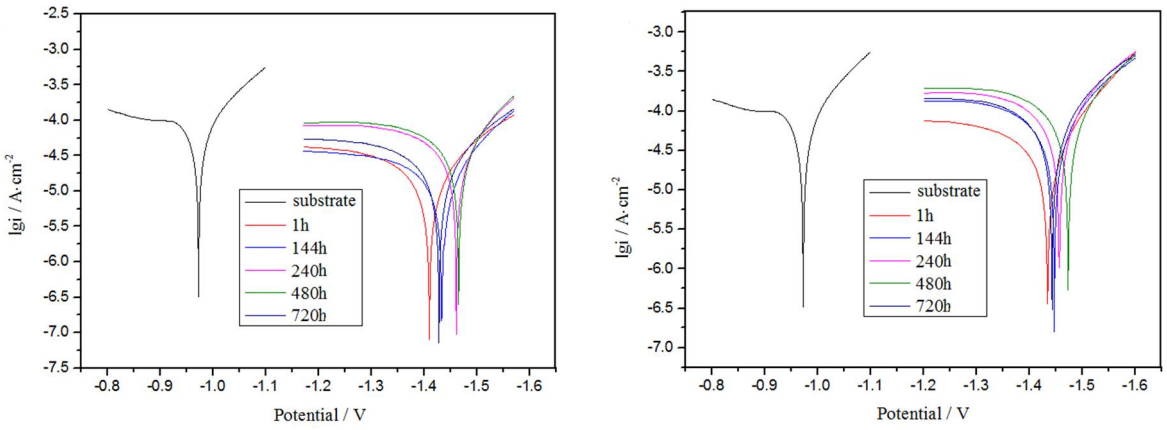

Figure 9. The tafel polarisation curves plot of Zn-Al coating and Zn- Al-Mg-TiO_2 composite coating in 3.5% NaCl solution at different times: (a)The tafel polarisation curves plot of Zn-Al coating; (b)The tafel polarisation curves plot of Zn- Al-Mg-TiO_2 coating

Table 1. Corrosion potential and current density of Zn-Al coating

Time	Ecorr/V	IcorrA·cm^{-2}
1h	-1.434	3.500E-5
144h	-1.447	7.668E-5
240h	-1.456	1.017E-4
480h	-1.473	1.104E-4
720h	-1.443	8.522E-5

Table 2. Corrosion potential and current density of Zn-Al-Mg-TiO_2 coating

Time	Ecorr/V	IcorrA·cm^{-2}
1h	-1.462	1.727E-5
144h	-1.440	1.92E-5
240h	-1.492	4.536E-4
480h	-1.495	5.138E-4
720h	-1.458	2.594E-5

3.5 Protective mechanism

The protective mechanism of Zn-Al-Mg-TiO_2 coating is similar to the Zn-Al coating. Fig.10 (b) is a schematic diagram of the protective mechanism of Zn-A-Mg-TiO_2 coating. At the initial stage of corrosion, the active metal zinc in the coating acts intense reaction as an anode, providing cathodic protection for substrate by consuming itself. At this time, the corrosion products of Al and Mg in the coating act together with the corrosion products of Zn to form a dense passivation film, the nanostructure of TiO_2 blocks the corrosion hole of the coating surface, so they can effectively blocks the intrusion channel of halogen ions and slows down the corrosion rate. In contrast, the protective mechanism of Zn-Al coating is shown in Fig. 3.10(a). Since there is no Mg to improve the passivation film and no TiO_2 to close the gaps, the compactness of passivation film structure is relatively poor. Therefore, a large number of corrosive media can still enter from the surface voids of the coating to corrode the internal materials of the coating with a faster rate. So the corrosion resistance is poor.

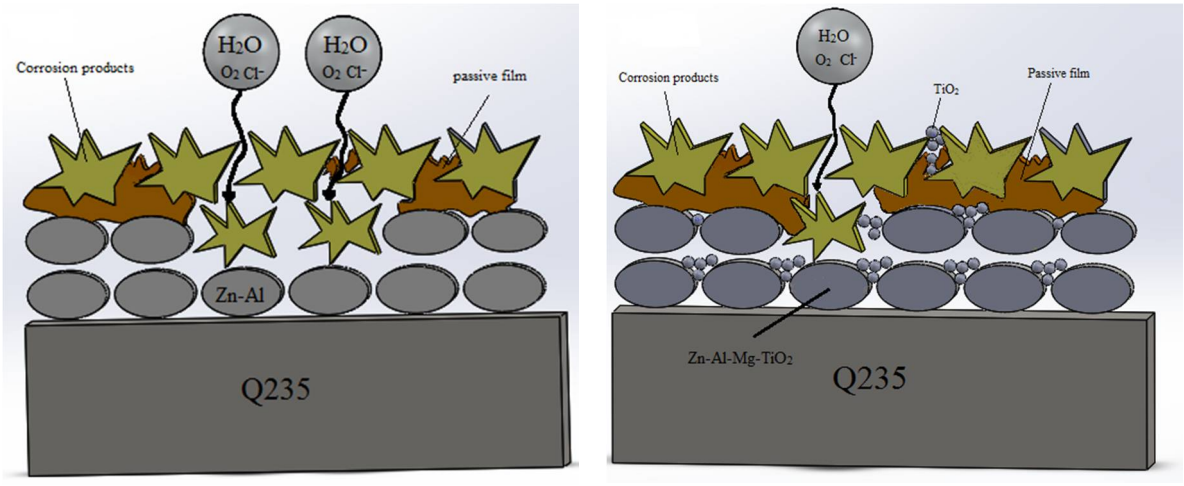

Figure 10. Schematic diagram of the protective mechanism of the two coatings: (a)Schematic diagram of the protective mechanism of the Zn-Al; (b)Schematic diagram of the protective mechanism of the Zn-Al-Mg-TiO2

4. Conclusions

(1) The surface of Zn-Al-Mg-TiO_2 composite coating with Mg and nano-TiO_2 is smoother. There are fewer pores and pits and the friction coefficient is 0.3629 which is lower than Zn-Al coatin. In addition, the scratch of Zn-Al-Mg-TiO_2 is more dense and uniform, so the coating has good wear resistance.

(2) The change trend of the corrosion rate of Zn-Al-Mg-TiO_2 coating in 3.5% NaCl solution is similar to the Zn-Al coating. Corrosion rate of the coating is gradually increased at the beginning of corrosion. As the immersion time increases, when the corrosion progresses to a certain extent, the corrosion rate stops increasing and begins to gradually decrease. However, under this trend, the corrosion current density of Zn-Al-Mg-TiO_2 coating is always lower than that of Zn-Al coating that indicate the Zn-Al-Mg-TiO_2 coating has better corrosion resistance.

(3) In 3.5% NaCl solution, a layer of grid-like floc corrosion product is formed on the surface of the Zn-Al-Mg-TiO_2 coating which can gather a lot of corrosion products to form a dense passivation film. It is found by experiment that the passivation film can effectively prevent Cl^- further intrusion and improves the corrosion resistance of the coating.

Author Contributions: S.W. developed an experimental plan. K.W. wrote the main part of the manuscript. K.W. and S.W. carried out the preparation of different composite materials and tested the mechanical properties. K.W. and G.W. performed characterization of the microstructure of the samples. K.W. and D.W. made the final typesetting of the article. S.W. summed up the article and conducted a final review.

Funding: This research was funded by the National Natural Science Foundation of China (No. 51872122, No. 51705199), Shandong Key Research and Development Plan of China (No.: 2016JMRH0218) and Taishan Scholar Engineering Special Funding (2016-2020).

References

1. Hideki, K.; Seiji, K. Long-term atmospheric corrosion properties of thermally sprayed Zn, Al and Zn-Al coatings exposed in a coastal area. Corrosion Science. 2013,76,35-41, doi:10.1016/j.corsci.2013.05.021.
2. Junfeng, G,; Guan,W,; Yuelin, N,; Lei, G,; Yongkang, Z,; Jiawei, L,; You, W. Preparation and corrosion resistance of chromium-free Zn-Al coatings with two different silane coupling agents. Surface and Coatings Technology. **2019**,366,1-6, doi:10.1016/j.surfcoat.2019.03.020.
3. Perez, A,; Billard, A,; Rébéré, C,; Berziou, C,; Touzain, S,; Creus, J. Influence of metallurgical states on the corrosion behaviour of Al–Zn PVD coatings in saline solution. Corrosion Science. **2013**,74,240-249, doi:10.1016/j.corsci.2013.04.048.
4. Mengxia, L,; Robert, M,; Igor, C. Corrosion and pitting of 6060 series aluminium after 2 years exposure in seawater splash, tidal and immersion zones, Corrosion Science. **2018**,140, 286-296, doi:10.1016/j. corsci.2018.05.036.
5. Weihua, L,; Ang, L,; Huiwen, T,; Dapeng, W. Controlled Release of Nitrate and Molybdate Intercalated in Zn-Al-Layered Double Hydroxide Nanocontainers towards Marine Anticorrosion Applications. Colloid and Interface Science Communications. **2018**,24,18-23, doi:10.1016/j.colcom.2018.03.003.
6. Wei, L,; Qian, L,; Mou-Cheng, L. Corrosion behaviour of hot-dip Al–Zn–Si and Al–Zn–Si–3Mg coatings in NaCl solution. Corrosion Science. **2017**,121,72-83, doi:10.1016/j.corsci.2017.03.013.
7. Shimpei, T,; Izumi, M,; Yu, S,; Michiyasu, T,; Masamitsu, M,; Nobuyoshi, H. Micro-electrochemical investigation on the role of Mg in sacrificial corrosion protection of 55mass%Al-Zn-Mg coated steel. Corrosion Science. **2017**,129,126-135, doi:10.1016/j.corsci.2017.07.020.
8. Monojit, D,; Arup, K. H,; Shiv, B. S. Morphology and properties of hot dip Zn–Mg and Zn–Mg–Al alloy coatings on steel sheet. Surface and Coatings Technology. **2010**,205, 2578-2584, doi:10.1016/j.surfcoat. 2010.10.006.
9. Caizhen, Y,; Haibing, L,; Tianping, Z,; Wanguo, Z,; Xiaodong, Y,; Wei, Ga. Effect of Mg content on microstructure and corrosion behavior of hot dipped Zn–Al–Mg coatings. Journal of Alloys and Compounds. **2016**,670,239-248, doi:10.1016/j.jallcom.2016.02.026.
10. Joung, H. L,; Sang, Y. L,; Seok, J. H. Synthesis of Zn–Mg coatings using unbalanced magnetron sputtering and theirs corrosion resistance. Surface & Coatings Technology. **2014**, 259,56–61, doi:10.1016/j.surfcoat. 2014.07.006.

11. Baghery, P,; Farzam, M,; Mousavi, A.B,; Hosseini, M. Ni-TiO_2 nanocomposite coating with high resistance to corrosion and wear. Surface&Coatings Technology. **2010**,204,3804—3810, doi:10.1016/j.surfcoat. 2010.04.061.

12. Chenglong, L,; Yueji, W,; Meng, W,; Weijiu, H,; Paul K. C. Electrochemical stability of TiO_2 nanotubes with different diameters in artificial saliva. Surface and Coatings Technology. **2011**, 206 63-67, doi:10.1016/j.surfcoat.2011.06.038.

13. Vlassis, L. Photonic crystal-assisted visible light activated TiO_2 photocatalysis. Applied Catalysis B: Environmental. **2018**,230,269-303, doi:10.1016/j.apcatb.2018.02.039.

14. Fei, Xu,; Tao, W,; HongYu, C,; James, B,; Alvin, M. M,; Limin, W,; Shuxue, Z. Preparation of photocatalytic TiO_2-based self-cleaning coatings for painted surface without interlayer. Progress in Organic Coatings. **2017**,113,15-24, doi:10.1016/j.porgcoat.2017.08.005.

15. Kyeong, S. M,; Ramalingam, M,; Young, A. S. Porphyrin Dye/TiO_2 imbedded PET to improve visible-light photocatalytic activity and organosilicon attachment to enrich hydrophobicity to attain an efficient self-cleaning material. Dyes and Pigments. **2019**,162,8-17, doi:10.1016/j.dyepig.2018.10.014.

16. Saravanan, N,; D. Shanthana, L,; Vignesh, T,; Mrudula, P,; Chandrasekaran, N,; Amitava, M. Antifouling and anti-algal effects of chitosan nanocomposite (TiO_2/Ag) and pristine (TiO_2 and Ag) films on marine microalgae Dunaliella salina. Journal of Environmental Chemical Engineering. **2018**,6, 6870-6880, doi:10.1016/j.jece.2018.10.050.

17. Jinxia, Z,; Mingxi, P,; Chuanbao, L,; Xiangping, C,; Jiangrong, K,; Tao, Z. A novel composite paint (TiO2/fluorinated acrylic nanocomposite) for antifouling application in marine environments. Journal of Environmental Chemical Engineering. **2016**,4,2545-2555, doi:10.1016/j.jece.2016.05.002.

18. Xianming, S,; Ning, X,; Keith, F,; Jing, G. Durability of steel reinforced concrete in chloride environments: An overview. Construction and Building Materials. **2012**,30,125-138, doi:10.1016/j. conbuildmat.2011.12. 038.

19. Ki, Y. A,; Ha, W. S. Chloride threshold level for corrosion of steel in concrete. Corrosion Science. **2007**,49,4113-4133, doi:10.1016/j.corsci.2007.05.007.

20. Hidekazu, T,; Saki, N,; Tatsuo, I,; Takenori, N. Simulating study of atmospheric corrosion of Zn-Al alloy coating in industrial zone: Structure and properties of zinc hydroxysulfate rust particles prepared in the presence of Al(III),.Advanced Powder Technology. **2019**,30,807-814, doi:10.1016/j.apt.2019.01.009.